https://doi.org/10.5194/egusphere-2026-5288
Preprint. Discussion started: 24 September 2026

Dome C migration in Antarctica during the last 800,000 years

Victor van Aalderen[1,2,3], Aurélien Quiquet[1,2], Christophe Dumas[1,2], Elisabeth Michel[1,2], Frederic Parrenin[3] and Catherine Ritz[3], Kevin Jiguet-Covex[1]

[1]Laboratoire des Sciences du Climat et de l'Environnement (LSCE), CEA, CNRS, UVSQ, Université Paris-Saclay, Gif-sur-Yvette, France

[2]Institut Pierre-Simon Laplace (IPSL), Université Versailles Saint-Quentin, Guyancourt, France

[3]Institut des Géosciences de l'Environnement (IGE), Université Grenoble Alpes, CNRS, IRD, INRAE, Grenoble INP, Grenoble, France.

Correspondence to: Victor van Aalderen (victor.van-aalderen@univ-grenoble-alpes.fr)

Abstract. The ice core extracted as part of the Beyond EPICA project is expected to provide the longest continuous climate record, reaching back at least 1.2 million years. However, the hypothesis that Dome C has remained stable over several glacial-interglacial cycles, which is a prerequisite for establishing a reliable age-depth relationship, remains unverified. Using the GRISLI2.0 ice sheet model, we perform an ensemble of 5 high-resolution nested simulations at 10 km × 10 km resolution to track the evolution of Dome C position over the past 800,000 years. Our results show that Dome C undergoes substantial displacements over time, strongly controlled by grounding line dynamics in the Aurora Subglacial Basin. Using a 1D ice flow model, we further demonstrate that these dome migrations can introduce age errors of several tens of thousands of years in the age-depth relationship, with the largest uncertainties affecting the oldest and deepest ice, precisely where the Beyond EPICA record is most critical.

Plain Language Summary: Ice cores from Dome C provide one of the longest climate records, and Beyond EPICA aims to extend it further. Interpreting these records requires knowing whether Dome C has remained fixed. Using an ice sheet model spanning 800,000 years, we show Dome C has shifted several km during glacial cycles, driven by grounding line migration in the Aurora Subglacial Basin. This displacement can introduce age errors of several tens of thousands of years when interpreting the ice-core record.

1 Introduction

Ice cores extracted from polar regions provide climate archives, enabling the reconstruction of Earth's climate over hundreds of thousands of years. They provide essential information about past atmospheric temperatures and the composition of the atmosphere, including greenhouse gas concentrations, which is essential for understanding the mechanisms governing our climate system. This is notably the case for the EPICA Dome C ice core, which offers a continuous climate record spanning the past 800,000 years (Jouzel et al., 2007). To further improve our understanding of the mechanisms driving long-term climate variability, the Beyond EPICA project recently successfully drilled a new ice core at the Little Dome C site (Chung et al., 2023; Lilien et al., 2021), with the aim to extend the climate record at least back to 1.2 million years.

https://doi.org/10.5194/egusphere-2026-5288
Preprint. Discussion started: 24 September 2026

One of the major challenges in interpreting ice cores lies in establishing an accurate chronology, that is, the relationship between the age of the ice and its depth, and also to determine its spatial origin and past trajectory (Parrenin et al., 2004). These are crucial for dating past climate events and interpreting the climatic and environmental signals preserved in the ice (Bouchet et al., 2023). For low snow accumulation sites such as Dome C (7-8 cm/yr, Stefanini et al., 2025), the relationship between age and depth is typically derived using simulations based on accumulation and ice flow models, constrained by glaciological and isotopic data (Bazin et al., 2013; Parrenin et al., 2017; Bouchet et al., 2023).

These models generally one-dimensional assume that the ice column is vertically stratified and that the position of the dome has remained stable over time. The assumption of stationarity for dome position has traditionally been widely accepted for sites like Dome C, where measured ice velocities are on the order of centimeters per year (Mouginot et al., 2017). However, other Antarctic domes have experienced significant divide migration, inferred from the geometry of internal radar layers, such as Talos Dome (~3.5 m yr^{-1}; Urbini et al., 2008) or Siple Dome (0.05–0.5 m yr^{-1}; Nereson & Raymond, 1998), demonstrating that significant movements can occur even where surface velocities are low. To better represent these slow but non-negligible movements, some studies have implemented 2.5D flow-tube models that capture both vertical and longitudinal ice-flow variations (Chung et al., 2025; Parrenin et al., 2004; Koutnik et al., 2016). But these models rely on a prescribed geometry, rather than one emerging from large-scale ice-sheet dynamics. They therefore miss the two-way coupling between whole-ice-sheet processes and the local flow regime at the dome.

Although Dome C is characterized by low ice flow velocities and minimal surface accumulation, its precise past displacement remains difficult to assess and the hypothesis of a stable dome position over the last million years remains unverified. Some studies based on shifts in precipitation patterns suggest a slight movement over the past century (Urbini et al., 2008). In addition, modelling experiments indicate that spatial variations in geothermal heat flux could lead to a migration of several tens of kilometres over longer timescales (Sutter et al., 2019). Furthermore, changes in ice dynamics and basal melting have been shown to affect the interpretation of ice core chronologies, as evidenced at Vostok (Parrenin et al., 2004), which could similarly apply to Dome C. More recently, Vittuari et al. (2025) showed, thanks to satellite observations, a migration of about 100 m a^{-1} at Dome C, likely linked to changes in accumulation distribution and shifts in the Byrd Glacier drainage basin.

More broadly, ice-sheet modelling has also been used to investigate dome migration in Greenland. Marshall and Cuffey (2000) found that the Summit divide could have shifted by as much as 150 km over the last 160 kyr. As a consequence, the ice surrounding the Summit drilling sites would have undergone changes in flowline direction and experienced non-negligible shear during the last deglaciation. This disturbed ice flow around the drilling sites complicates the interpretation of the GRIP and GISP2 ice cores, as the analyzed ice did not necessarily follow a simple, vertical trajectory.

https://doi.org/10.5194/egusphere-2026-5288
Preprint. Discussion started: 24 September 2026

As a result, past dome migration can perturb the age/depth relationship by introducing horizontal advection, meaning that ice at a given depth may no longer correspond to the location where it originally accumulated (Chung et al., 2025; Parrenin et al., 2004). This dynamic complicates stratigraphic interpretations and calls for more realistic flow models to correct for deformation induced by such displacements (Parrenin et al., 2004).

In this context, more detailed studies are needed to quantify any potential displacement of Dome C over multiple glacial-interglacial cycles, and to assess whether such movements may have influenced the age-depth relationship. To explore this issue, we conducted a series of numerical simulations of the Antarctic Ice Sheet (AIS) using the GRISLI2.0 model, covering the last 800,000 years. In order to better resolve the local ice sheet dynamics in the Dome C region, the continental-scale simulations were refined using a nested high-resolution domain centred on Dome C. These simulations allow us to track the spatio-temporal evolution of the Dome C position at higher resolution and to quantify dome migration and its impact on the age-depth relationship using a 1D ice flow model.

2 Methods

2.1 GRISLI ice sheet model

In this study, we used the GRISLI2.0 ice sheet model (hereafter GRISLI), a three-dimensional thermomechanically coupled model that simulates the evolution of ice sheets, with a horizontal resolution of 40 km × 40 km. GRISLI has been validated for the Antarctic ice sheet over glacial/interglacial timescales (Quiquet et al., 2018) and has been applied in various model intercomparison efforts for both Antarctica and Greenland (e.g., Goelzer et al., 2020; Seroussi et al., 2020) and other paleo ice sheet (Quiquet et al., 2021; van Aalderen et al., 2024). In the following, we provide a description of the main components of the ice sheet model, but a full description of GRISLI can be found in Quiquet et al. (2018).

GRISLI solves the ice flow using a hybrid approach following the shallow-ice approximation (SIA) accounting for vertical shearing, while the shallow-shelf approximation (SSA) is applied as a sliding law and for the ice shelves. Grounding line migration is computed using the analytical solution of Schoof (2007) and calving occurs when ice thickness falls below a threshold of 250 m. The model includes isostatic adjustment through an elastic lithosphere-relaxed asthenosphere scheme and operates on a grid at 40 km horizontal resolution with 21 vertical layers. Initial ice sheet geometry, bedrock elevation, and ice thickness are taken from the BedMachine Antarctica v3 dataset (Morlighem et al., 2022) assuming that this present-day state corresponds to an isostatic equilibrium. Geothermal heat flux follows Haeger et al. (2022).

https://doi.org/10.5194/egusphere-2026-5288
Preprint. Discussion started: 24 September 2026

For temperate-based grounded ice, we apply a Budd-type basal friction law (Brondex et al., 2017), expressed as τb = -β * ub, where ub is the basal ice velocity and β is the basal drag coefficient. The latter depends linearly on the effective pressure N, such that β = Cf * C_sed * N. The coefficient Cf is an internal uniform parameter and C_sed is a two-value parameter to account for different local bed rheology. Typically, C_sed is set to 1 where the ice-free isostically rebounded bedrock is above present-day sea level. Elsewhere, we use a lower value to artificially account for reduced friction in regions with high sediment deposits, which is an important parameter to properly represent the glacial–interglacial cycles. This approach assumes that areas currently below sea level have accumulated thicker sediment layers, while regions above sea level exhibit thinner sediment cover due to long-term glacial erosion.

To implicitly represent the effects of ice anisotropy, GRISLI incorporates a flow enhancement factor (Ef; Quiquet et al., 2018), which also affects both the SSA and SIA velocities. When Ef=1, it corresponds to isotropic ice and SIA and SSA are not modified. For EfSIA>1 the SIA velocities are increased, while the SSA velocities are reduced. The SSA enhancement factor is linked to the SIA enhancement factor EfSIA. For example, when EfSIA=2, EfSSA=0.45, when EfSIA=3, EfSSA=0.267, and when EfSIA=5, EfSSA=0.12 (Ma et al., 2010)

Surface ablation is simulated using a Positive Degree Day (PDD) approach adapted from Tarasov and Peltier (2002). Melt rates are calculated for snow and ice based on the mean summer surface air temperature. Snow accumulation is estimated from monthly precipitation totals, restricted to periods when average temperatures remain below 0 °C, and is further corrected according to surface temperature using a Clausius–Clapeyron relationship.

Atmospheric and oceanic temperatures, precipitation, and salinity are interpolated onto the GRISLI model grid using bilinear interpolation. To reconcile differences in topography between the GCMs and the reference climate model RACMO2.4p1, a uniform lapse rate correction (7 °C/km) is applied to the interpolated near-surface air temperature fields. This lapse rate is also used to adjust temperatures during modelled changes in ice surface elevation, capturing the altitude temperature feedback.

Ocean-induced basal melting beneath floating ice shelves is computed with the nonlocal quadratic parametrization suggested in ISMIP (Jourdain et al., 2020). The melt rate (OM) is expressed as:

$$OM = \frac{K_t \times \rho_w \times C_w}{\rho_i \times L_f} \left|T_o - T_f\right| \left(T_o - T_f\right) \qquad (1)$$

Here, Kt is the thermal exchange coefficient, ρw and ρi are the densities of seawater and ice respectively, Cw is the specific heat of seawater, and Lf is the latent heat of fusion for ice. To is the 3D ocean temperature, and Tf the local freezing point, which is a function of salinity and is computed using the parameterization described in Beckmann and Goosse (2003). Since GCMs do not provide data beneath ice shelves, these gaps were filled based on the values of the nearest neighboring grid cells within a given oceanic sector.

https://doi.org/10.5194/egusphere-2026-5288
Preprint. Discussion started: 24 September 2026

2.2 Climate forcing anomalies

To generate past climatic forcings we first constructed Last Glacial Maximum (LGM, ~21 ka) anomalies with respect to the pre-industrial (PI) from 10 different available PMIP3 and PMIP4 climate simulations. These include IPSL-CM5A, CCSM4, FGOALS-g2, IPSL-CM5A2, GISS, MIROC-ESM, MIROC-ES2L, MPI-ESM-P, MPI-ESM1.2, and MRI-CGCM3 (Adloff et al., 2018; Yukimoto et al., 2012; Sueyoshi et al., 2013; Voldoire et al., 2013; Ullman et al., 2014; Zheng and Yu et al., 2013; Dufresne et al., 2013; Sepulchre et al., 2020; Hajima et al., 2020; Mauritsen et al., 2019).

These anomalies are added on top of the reference present-day climate, which comes from RACMO2.4p1 (van Dalum et al., 2025) for the atmosphere and from the observation ISMIP dataset from the ocean (Jourdain et al., 2020), using a time-evolving weighing index (see in the supplementary for more information, and see fig 1). The two indexes, one for the atmosphere and one for the ocean, show a value of 1 at the LGM and 0 at present. When the index is equal to 1 the full anomaly of the PMIP model is added to RACMO2.4p1 and the present-day ocean forcing, while when the index value is 0, the reference atmospheric and oceanic forcings are used. The atmospheric index was constructed using the EPICA Dome C ice core record (Jouzel et al., 2007), based on the temporal evolution of the deuterium isotope over the past ~800,000 years. The chronology follows the AICC2023 age model (Bouchet et al., 2023). In parallel, the oceanic index was derived from the stack of Chandler and Langebroek, 2024, which reconstructs the ocean bottom temperature over the last 800,000 years. We synchronized this marine record to the AICC2023 timescale using the AnalySeries software (Paillard et al., 1996).

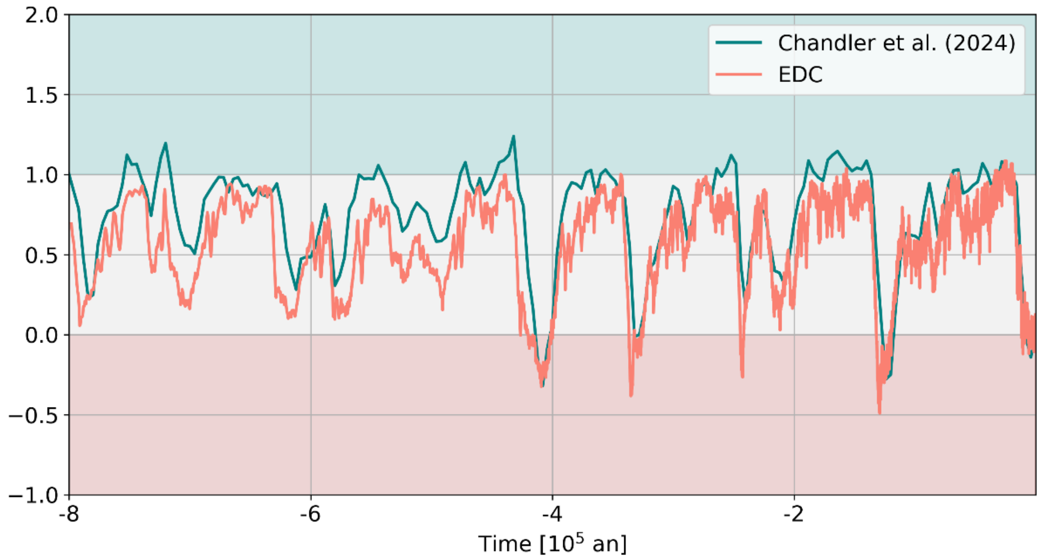

Figure 1: Evolution of the atmospheric index (in red, Jouzel et al., 2007) and the oceanic index (in green, Chandler et al., 2024) over the past 800,000 years

https://doi.org/10.5194/egusphere-2026-5288
Preprint. Discussion started: 24 September 2026

2.3 Dome C algorithm

We developed an algorithm to identify and track the position of Dome C over the last 800,000 years, applied offline to the model output. At each output time step, candidate dome locations are identified as local maxima in surface elevation (search radius of 20–50 km) with ice velocity below 1 m yr^{-1} and low surface slope. Because the model's spatial resolution prevents slopes from reaching values close to zero, a slope threshold is used, starting at 0.5 m km^{-1} and increased in steps of 0.01 m km^{-1}, up to 1.5 m km^{-1}, until a candidate is found. When several candidates satisfy these criteria, the one closest to the dome position at the previous output time step is selected, ensuring a continuous trajectory. Model outputs are available every 10,000 years. To avoid huge jumps between successive detections, we impose a maximum displacement of ~60 km between two outputs, corresponding to an average migration rate of ~6 m yr^{-1}, consistent with migration rates reported for other Antarctic domes (Urbini et al., 2008; Nereson & Raymond, 1998). We note that this threshold may underestimate migration rates during rapid transitions such as deglaciations.

2.4 1D ice flow modelling

To compute a first approximation of the age–depth relationship at the simulated position of Dome C, we use the 1D ice flow model developed by Parrenin et al. (2007), which remains the standard approach used to derive the thinning function for the EDC ice core chronology, including the most recent AICC2023 chronology (Bouchet et al., 2023). This model assumes that ice flow is primarily vertical at the dome and that horizontal velocities are negligible, an assumption that is well supported in the Dome C region (Parrenin et al., 2007). The vertical ice velocity at the normalized position ζ (0 is surface and 1 is ice-bedrock interface) within the ice column is written as:

$$u_\zeta(\zeta, t) = \frac{-1}{H(t)}\left[m(t) + \left(a(t) - \frac{\partial H(t)}{\partial t} - m(t)\right)\omega(\zeta) + \zeta\frac{\partial H(t)}{\partial t}\right] \quad (2)$$

where ω(ζ) is a Lliboutry-type velocity profile (Lliboutry, 1979), H(t) is the ice thickness, m(t) the basal melt rate and a(t) the surface accumulation rate.

Once the vertical velocity is computed, the position of each ice layer is updated at every time step as follows:

$$\zeta(t + dt) = \zeta(t) + u_\zeta \cdot dt \quad (3)$$

Finally, the pressure exerted by the upstream ice causes the ice thickness to vary through time. In the 1D flow model, this new thickness is computed as:

$$\Delta z(t + dt) = \Delta z(t) \times (1 + \dot{\varepsilon}_{zz} \cdot dt) \quad (4)$$

ε_{zz} with the thinning rate of this layer.

https://doi.org/10.5194/egusphere-2026-5288
Preprint. Discussion started: 24 September 2026

A full description of the 1D ice flow model can be found in Parrenin et al. (2007).

By tracking each ice layer from its deposition at the surface to the present day, the age-depth relationship is obtained directly. According to this model, the depth of an ice layer in the core depends on the surface accumulation rate, the basal melt rate, and variations in ice thickness over time.

Unlike Parrenin et al. (2007), where ice thickness, basal melt rate and accumulation are estimated through a simplified conceptual model, we use here directly the outputs of the GRISLI ice sheet model. These outputs provide at each time step the simulated ice thickness variations, the surface accumulation corrected for changes in surface elevation, as well as the basal melt rate computed from the basal temperature and the friction of ice against the bedrock.

3 Experimental setup

3.1 Initial states: present-day calibration

To initialise the thermodynamical state of the AIS and account for uncertainties related to key model parameters, we perform a Latin Hypercube Sampling (LHS) ensemble consisting of 300 simulations, each simulation spanning 150,000 years under present-day climatic conditions. The ensemble explores variations in six parameters that play a crucial role in ice sheet dynamics:

- The enhancement factor (Ef), varied between 1 and 5, which increase shear-stress-driven deformation and therefore affects the velocity field (Quiquet et al., 2018).
- The viscosity coefficient for the non-linear part (Sf3), which impact the ice viscosity.
- The basal drag coefficient (Cf), tested within the range 0.05 to 0.5 an/m, which directly controls the resistance to sliding at the ice base.
- The sediment specific basal drag coefficient (Csed), ranging from 0.1 to 1.0, which governs basal sliding in regions with sediment.
- The till conductivity (Ko), varied between 0.0005 and 0.005 m/an, which affects the effective pressure at the bed and consequently modulates basal sliding (Quiquet et al., 2018).
- The thermal exchange coefficient (Kt), ranging from 11.500 to 17.500 m/an/°C, which impacts ice shelf basal melt rates (Pollard and DeConto, 2012)

The spin-up simulations are forced with atmospheric conditions from the RACMO2.4p1 climatology and oceanic conditions from the ISMIP6 climatology (Jourdain et al., 2020). The 150,000-year simulations explore a wide range of parameter

https://doi.org/10.5194/egusphere-2026-5288
Preprint. Discussion started: 24 September 2026

combinations (see Figure 2), ensuring a broad sampling of the model parameter space. At the end of these simulations, we select the ten parameter sets that yield the lowest root mean square error (RMSE, see Fig 2) when compared to present-day ice thickness observations (Morlighem et al., 2022).

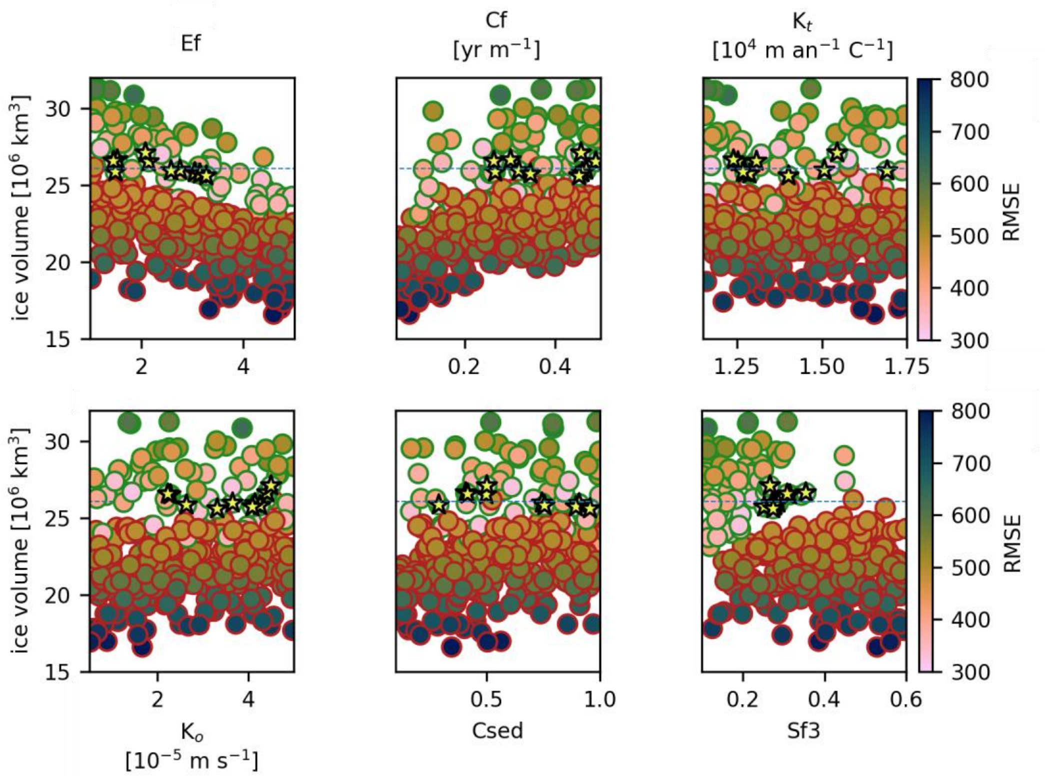

Figure 2: Ice thickness root mean square error respective to observations in the parameter space for the 300 model members. The stars show the ten best RMSE and the blue line shows the actual observed total ice volume (Morlighem et al., 2022). The green contour indicates the presence of the WAIS at the end of the equilibrium simulation, while the red contour indicates a complete retreat of WAIS.

3.2 Reference 800,000 year transient experiments

We performed 100 transient experiments covering the last 800,000 years, using the 10 best parameter combinations found in present day calibration forced by the 10 GCM climate anomalies weighted by the temporal indexes (see Section 2.2). According to stable isotope records, 800,000 years before present corresponds to a glacial period. However, for simplicity, we used as initial ice sheet states for our transient simulations those obtained from the equilibrium simulations, which correspond to interglacial conditions. The first glacial–interglacial cycle of our transient simulations is therefore interpreted as an adjustment phase, during which the model gradually adapts to the abrupt shift from interglacial to glacial forcing. After roughly 200,000 yr, the simulated ice sheet becomes independent of the initial conditions (displaying a consistent pattern of dome

https://doi.org/10.5194/egusphere-2026-5288
Preprint. Discussion started: 24 September 2026

displacement regardless of the spin-up used) and the subsequent evolution reflects the transient response to the applied climatic forcing (see Figure S1).

3.3 Nested 800,000 years transient experiments

To provide greater spatial detail in the Dome C region, the continental-scale simulations at 40 km resolution are refined using a nesting approach (following broadly the same method as presented in Halberstadt and Balco, 2026), enabling high-resolution simulations over a restricted domain while maintaining dynamical consistency with the large-scale simulation. The high-resolution domain covers the Dome C region at a resolution of 10 km × 10 km and was defined to encompass grounding line migrations in both the Wilkes and Aurora subglacial basins (Fig 3).

Boundary conditions applied at the edges of the nested domain (i.e. ice thickness, surface elevation, basal temperature, ice velocity, and basal friction) are extracted from the continental simulations, which serve as the nest-driving simulation. These conditions, available as snapshots every 10,000 years between -800 and -21 kyrs, and every 500 years after, are linearly interpolated between two successive time steps to ensure a temporally continuous forcing. To avoid dynamical discontinuities at the interface between the high-resolution domain and the driving simulation, a smootherstep function is applied over a buffer zone of 10 pixels along the domain edges, ensuring a smooth transition between the forced boundary conditions and the free dynamics in the interior of the domain.

Prior to launching the transient experiments covering the whole simulated period, an equilibration phase of 50,000 years is performed under PI conditions to allow the model to adapt to the new domain and reach a quasi-steady state at the higher resolution.

https://doi.org/10.5194/egusphere-2026-5288
Preprint. Discussion started: 24 September 2026

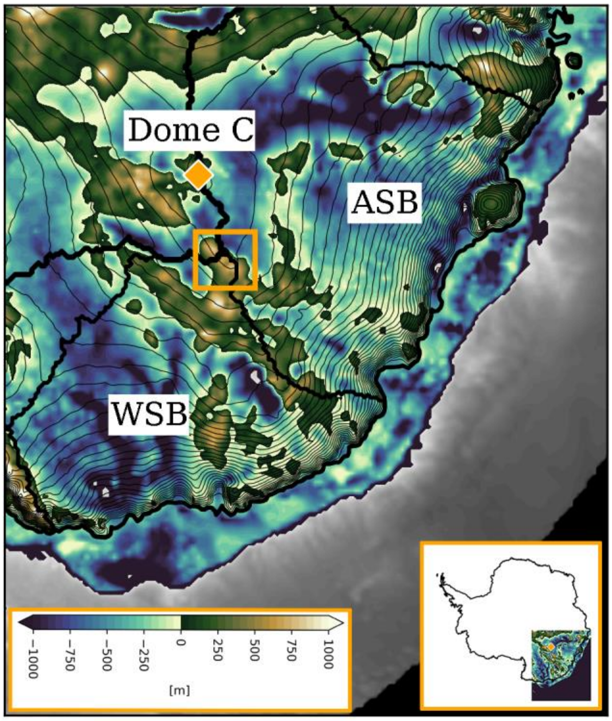

Figure 3: Nested simulation domain. The orange diamond shows the present-day position of Dome C, and the orange square shows the zone where the simulated position of Dome C is located at the start of the 5 high-resolution simulations (i.e., after the 50,000-year zoom equilibrium spin-up). ASB and WSB denote the Aurora Subglacial Basin and Wilkes Subglacial Basin, respectively.

4 Results

4.1 Simulated Antarctic ice volume over the last 800,000 years

Figure 4a shows the evolution of AIS volume over 800,000 years of simulation. The results highlight a large variability in ice volume between glacial and interglacial periods, especially after 400,000 years, with maximum fluctuations exceeding 10 million km³. In addition, the simulations show a strong dependency of the simulated ice volume on the choice of the GCM used to force GRISLI. Differences in total ice volume can exceed 5 million km³, particularly during glacial periods. However, this spread between forcings is generally less pronounced during interglacial periods, since all the simulations use the same interglacial climate reference state (RACMO2.4p1).

Out of 100 simulations (10 parameter sets × 10 GCMs), 76 show a final root mean square error (RMSE) below 360 m compared to present-day ice thickness (Morlighem et al., 2022). Among these, 10 simulations reach an RMSE below 400 m at the LGM compared to the GLAC-1D reconstruction (Tarasov et al., 2012; Abe-Ouchi et al., 2015), and 48 simulations remain under

https://doi.org/10.5194/egusphere-2026-5288
Preprint. Discussion started: 24 September 2026

450 m, indicating a good representation of ice volume and extent in our simulations over at least the last 21,000 years. However, all simulations underestimate the grounding line advance in the eastern part of the Ross Sea (see Figure 4b).

The simulations showing the greatest ice extent during glacial periods are those forced with the largest ocean temperature anomalies (i.e., more than 2°C difference between glacial and interglacial periods; Figure 4b and Figure S2). This suggests that increased ocean cooling leads to a greater advance of the grounding line, and therefore to a larger total ice volume. These results highlight the critical role of the ocean to drive the AIS volume and geometry.

Moreover, we show that some simulations lose the West Antarctic Ice Sheet (WAIS) during the interglacials at 400 kyr and 127 kyr. Such simulations are those forced by GCMs showing a subsurface ocean temperature warming anomaly exceeding 0.7°C in the WAIS basin, namely CCSM4, MIROC-ESM, MIROC-ES2L, MPI-ESM-P, MPI-ESM1.2, and MRI-CGM3 (see Fig. S2), regardless of the fixed physical parameters. All other models do not show a complete WAIS retreat over the last million years, owing to a glacial/interglacial anomaly that is too weak. This identifies a warming threshold that must not be exceeded in order to preserve the WAIS.
Taken together, this initial series of experiments provides a global range of plausible reconstructions of AIS volume and extent over the past 800,000 years, and can be used for further investigation into the long-term evolution and potential migration of Dome C.

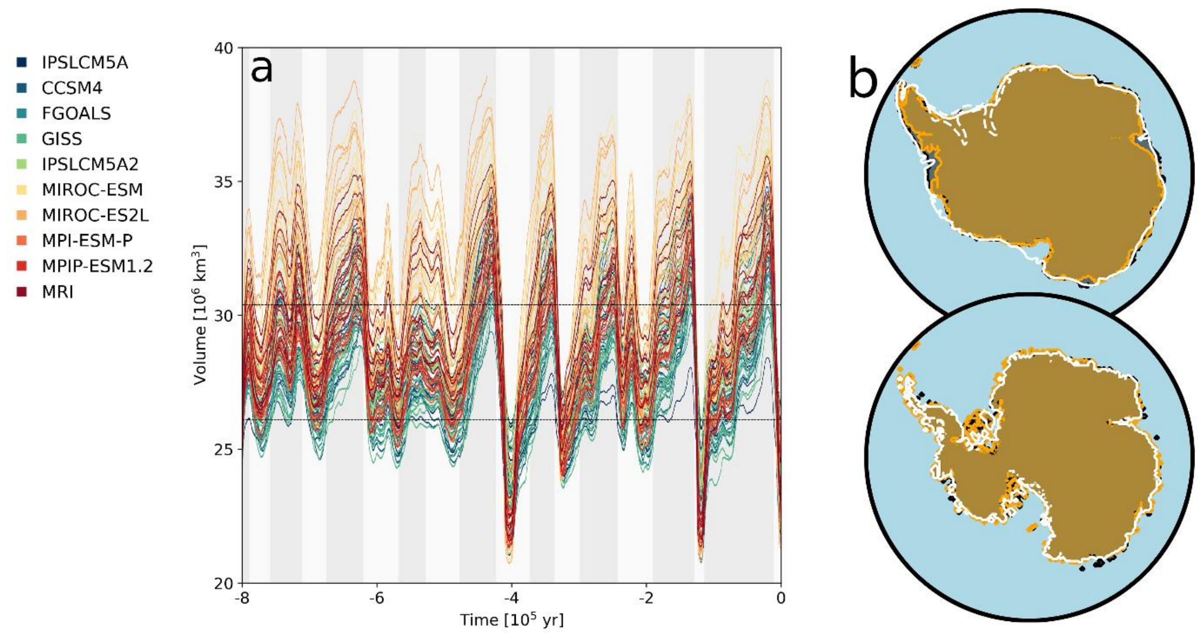

https://doi.org/10.5194/egusphere-2026-5288
Preprint. Discussion started: 24 September 2026

Figure 4: a: Simulated total ice sheet volume evolution over the last 800,000 yr for the 100 transient ensemble members. The two horizontal black lines come from the GLAC-1D reconstruction and current observations (Morlighem et al., 2022). b : top : maximum (in black) and minimum (in orange) extension of the LGM (-21ka) ice sheet according to the 10 simulations among the 100 with the lowest RMSE compared with observations (in white, Bentley et al., 2014). bottom: same as top but for the present-day ice extent compared with observations (Morlighem et al., 2022)

4.2 Simulated Dome C position over the last 800,000 years

Among the 100 continental simulations performed, the 5 best were selected according to three criteria. The first concerns the simulated ice volume and ice extend at the end of the 800,000-year simulation, compared to present-day observations. The second relates to the geometry of the ice sheet at the LGM, evaluated against the GLAC-1D and ICE-6G reconstructions. The third criterion is the presence of an ice dome within a 200 km radius of the present-day Dome C location at the end of the simulation. These 5 simulations were then restarted on the high-resolution nested domain described above, allowing for a better representation of the local ice sheet dynamics and Dome C displacements over the past 800,000 years, following the same climate forcing method than continental simulations.

Figure 5 shows the evolution of ice volume in the high-resolution domain over the past 800,000 years, compared to the LGM ice volume reconstructed by GLAC-1D and to present-day observations. The simulations correctly reproduce the amplitude of ice volume variations between glacial and interglacial periods, remaining within the bounds defined by these two references.

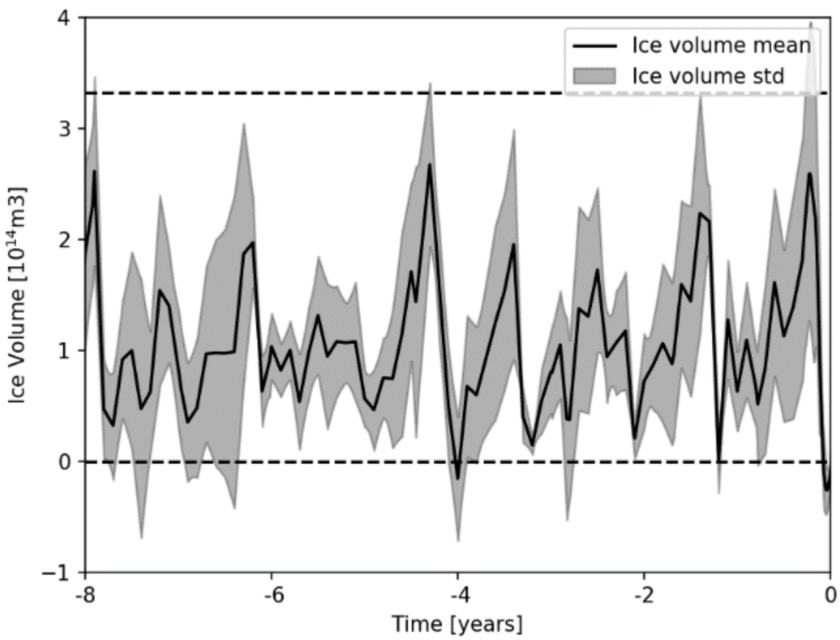

https://doi.org/10.5194/egusphere-2026-5288
Preprint. Discussion started: 24 September 2026

Figure 5: Mean ice volume evolution over time for the 5 nested simulations, expressed relative to the initial ice volume, and compared to present-day observations (Morlighem et al., 2022) and the GLAC-1D LGM reconstruction (dotted line).

Among all these simulations we used our dome detection algorithm to find and track the Dome C position (see Section 2.3). Figure 6 shows the density of Dome C presence throughout glacial/interglacial cycles, the LGM position (blue circle) and the ended position (orange circle).

First, the simulated dome position at the start of the 5 simulations is located approximately 150 km from the present-day Dome C position, towards the Wilkes Basin coast (See Figure 6 and 3). This offset is maybe due to the model's resolution limitations (10 km) and to the imperfect representation of bedrock topography at this scale. It may potentially introduce biases in the estimation of absolute dome displacements, due to slightly different bedrock conditions and local climate compared to the actual site. However, the simulations provide an estimate of the amplitude of dome displacements over glacial-interglacial cycles, even though the simulated absolute position remains subject to uncertainties inherent to the model limitations.

Secondly, we observe that the position of Dome C varies over time, evolving around its original location with a maximum displacement ranging from approximately 80 km (depending on the simulation). The simulations reveal also that the dome oscillates between two preferential positions, one during interglacial periods and another during glacial periods. In three of the five simulations, the glacial dome position is located several tens of kilometres towards the interior of East Antarctica relative to its interglacial position. This retreat is primarily driven by the advance of the grounding line during glacial periods, which generates a higher surface gradient, increases ice flow velocities, and consequently drives the dome position towards the East Antarctic interior.

In the two remaining simulations, both forced by FGOALS, the dome is instead shifted to the east during glacial periods relative to its interglacial position. This difference is explained by a subsurface ocean temperature anomaly that is opposite in sign compared to the other GCMs, where FGOALS simulated a slight warming of approximately 0.1°C in the Aurora and Wilkes basins during glacial periods relative to interglacial, which modifies the grounding line dynamics and, consequently, the dome position.

https://doi.org/10.5194/egusphere-2026-5288
Preprint. Discussion started: 24 September 2026

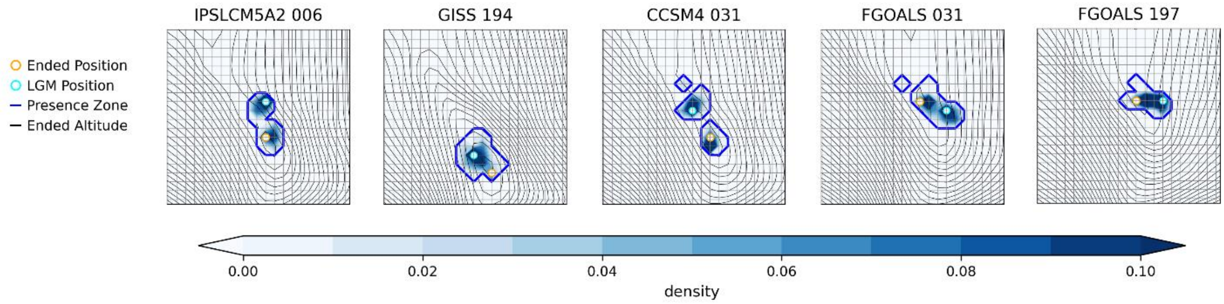

Figure 6: LGM position (blue circle) and final position (orange circle) of Dome C according to the 6 nested simulations. The density of presence over the 800,000 years is illustrated by the blue color bar. The blue contours represent the surface of presence during the simulation. The grey grid illustrates the model resolution, with each grid cell corresponding to 10 km × 10 km. The title shows the climate forcing and the ID number of the LHS member. The limits of the frame are the orange square shown in the fig 3.

Using the high-resolution nested simulations and the simulated dome positions, we computed the age-depth relationship using the 1D ice flow model described in section 2.4. In a first step, the age-depth relationship was computed assuming the dome to be fixed at its initial position. In a second step, the 1D model was run by tracking the dome position over time. Comparing these two approaches allows us to quantify the impact of dome migration on the age-depth relationship. The 1D ice flow model requires as input the temporal variations of ice thickness, surface accumulation and basal melt rate. In order to remove the bias introduced by the simulated initial dome position, which differs by approximately 150 km from the actual Dome C location, we follow the approach of Marshall and Cuffey (2000) by expressing dome displacements relative to their present-day position. The forcing fields for the 1D model are therefore extracted not at the absolute simulated dome position, but at the actual Dome C location offset by the relative displacement vector of the simulated dome at each time step.

Figure S3 shows the age-depth relationship for the fixed dome (blue curve) and mobile dome (orange curve) configurations. A first notable result is the significant spread, between the 5 simulations, in the age computed at the base of the ice core across simulations. Two simulations yield ages exceeding 1.2 million years (IPSLCM5A2_006 and GISS_194), two others reach approximately one million years (FGOALS_031 and CCSM4_031), and one simulation does not exceed one million years (FGOALS_197). These differences result from the combined influence of several factors controlling both the rate at which ice layers migrate towards the bedrock and the basal melt rate at the base of the ice sheet.

Figure 7 shows the difference in the age-depth relationship between the fixed dome and mobile dome. In the upper half of the ice core, dome displacements have a limited impact on the chronology, with maximum age differences of the order of 10,000 years. In contrast, in the lower half of the core, some simulations show differences exceeding 100,000 years between the two configurations. These large discrepancies are partly explained by the fact that the mobile dome position can be located in areas

https://doi.org/10.5194/egusphere-2026-5288
Preprint. Discussion started: 24 September 2026

where the basal melt rate is significantly higher than at the fixed position, leading to greater ice loss at the base of the column. In some cases, differences in basal melt rate of up to 0.6 mm/yr are observed between the mobile and fixed dome positions. These results highlight the large uncertainty affecting old ice ages, directly linked to our limited knowledge of basal melting beneath the ice sheet.

In order to isolate the respective contributions of ice thickness variations, surface accumulation and basal melt rate to the computed error in the age-depth relationship, we performed three additional sensitivity experiments using the 1D ice flow model. In each experiment, a single variable is taken from the mobile dome position while the two others are held at their fixed dome values:

- H(t) taken from the mobile dome position, a(t) and m(t) from the fixed dome position, in order to isolate the role of ice thickness variations (exp_dh).
- a(t) taken from the mobile dome position, H(t) and m(t) from the fixed dome position (exp_acc).
- m(t) taken from the mobile dome position, H(t) and a(t) from the fixed dome position (exp_bmelt).

Figure S4 shows the results of the three complementary sensitivity analyses. First, as discussed above, the age error at the base of the ice core is primarily driven by differences in basal melt rate between the fixed and mobile dome positions (see Fig S4c). Secondly, surface accumulation has only a minor impact on the age error, due to the weak precipitation gradient (< 5 mm/yr) within the dome migration zone. However, the FGOALS_031 simulation represents a notable exception, because the dome migrates towards regions with accumulation differences of up to 15 mm/yr, which accounts for the larger contribution of accumulation to the computed age error in this case. Finally, when ice thickness variations between the two positions exceed 500 metres (Fig. S5 and S4b), they have a non-negligible impact on the age error computed by the 1D flow model throughout the entire ice core, as illustrated by the GISS_194 and CCSM4_031 simulations. These two simulations exhibit large ice thickness variability in the Dome C sector, primarily associated with subsurface ocean temperature anomalies in the Wilkes and Aurora basins that are significantly larger than in the other simulations, producing strong variation in the grounding line position between a glacial and interglacial state. This result highlights the potential role of grounding line dynamics in controlling the position of Dome C.

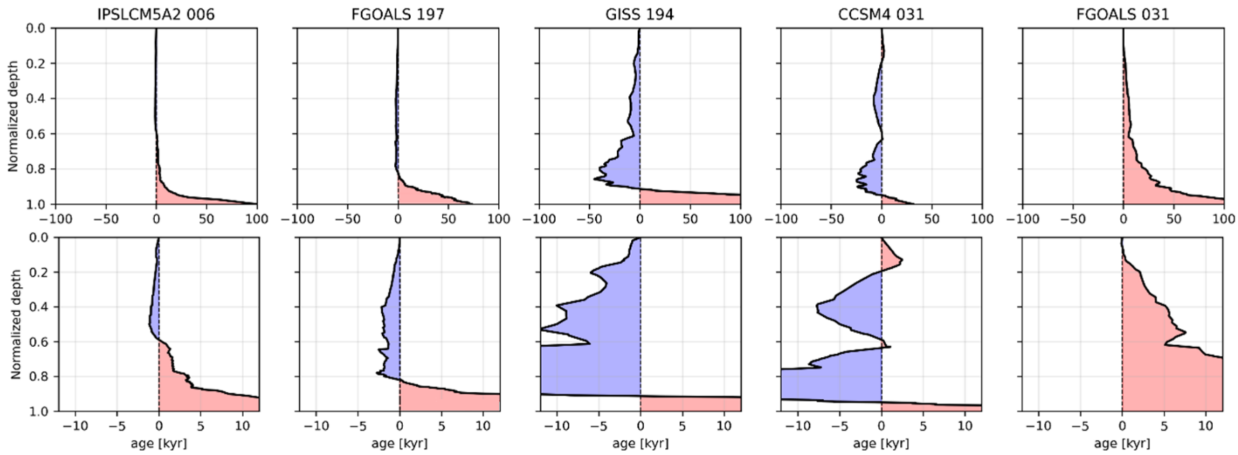

Figure 7: (top) Age difference as a function of normalized depth between the fixed and mobile dome. A positive value indicates that assuming a fixed dome leads to an overestimation of the ice age, while a negative value indicates an underestimation. (bottom) Same as the top panel, but with the x-axis restricted to -10 kyr, 10 kyr to better illustrate the small age differences in the upper half of the ice core.

4.3. What drives Dome C migration over the past 800,000 years?

A strong correlation is observed between the displacement of Dome C and the increase in ice volume, highlighting the key role of grounding line dynamics in controlling Dome C position. To further investigate this relationship, we designed three new nested simulations using the IPSLCM5A2 forcing and physical configuration n°006 (i.e. our best simulation, respect to the LGM and to the observed reconstructions). These experiments consisted of no longer imposing the Schoof (2007)' ice flux at the grounding line in order to make it more stable:

- Everywhere (experiment: no flux gl),
- across the entire Antarctic ice sheet except except in the Wilkes Subglacial Basin (gl WSB),
- across the entire Antarctic ice sheet except except in the Aurora Subglacial Basin (gl ASB),

Figure 8 presents the results of these new experiments compared to the reference simulation. When the grounding-line flux is no longer imposed around the AIS or in the WSB, the algorithm fails to identify a dome throughout the entire simulation. This reflects a fundamentally different ice-sheet geometry in this region, lacking the localized surface maximum and near-zero slope that define a dome under the reference configuration. In addition, the surface gradient at the expected dome location shows little temporal variation, despite changes in atmospheric temperature and precipitation patterns, indicating an absence of any detectable divide migration signal to track in this experiment. Furthermore, when the grounding line flux is allowed only in the ASB, the model reproduces a behaviour very similar to the reference simulation. This suggests that the grounding line dynamics in ASB play a central role in driving the simulated shifts in the position of Dome C. Previous studies, using

https://doi.org/10.5194/egusphere-2026-5288
Preprint. Discussion started: 24 September 2026

marine geological and geophysical data (Gulick et al., 2017) or modelling approaches (Hayden et al., 2025), demonstrated that the extent of the ASB can be sensitive to climatic variations. Therefore, it is highly likely that climate fluctuations during glacial and interglacial cycles affected the position of the grounding line in the ASB, and consequently influenced the location of Dome C.

Other factors may also influence the position of Dome C, such as changes in precipitation patterns, as suggested by Urbini et al. (2008), or changes in bedrock topography. We tested the sensitivity of the algorithm to bedrock changes in a series of low-resolution experiments and found limited impact on the detected dome position (not shown). To further investigate the role of precipitation, we conducted a new experiment prescribing a temporally constant precipitation pattern in the Dome C region while suppressing the ice flux across the grounding line in the ASB, in order to isolate the impact of these factors (experiment Acc_Const, see Fig. 5). As with the WSB and AIS experiments, no dome is detected throughout this simulation. Because this outcome is identical to that obtained when suppressing the grounding-line flux alone, this suggests that the disappearance of the dome is primarily driven by grounding-line dynamics rather than by precipitation pattern changes.

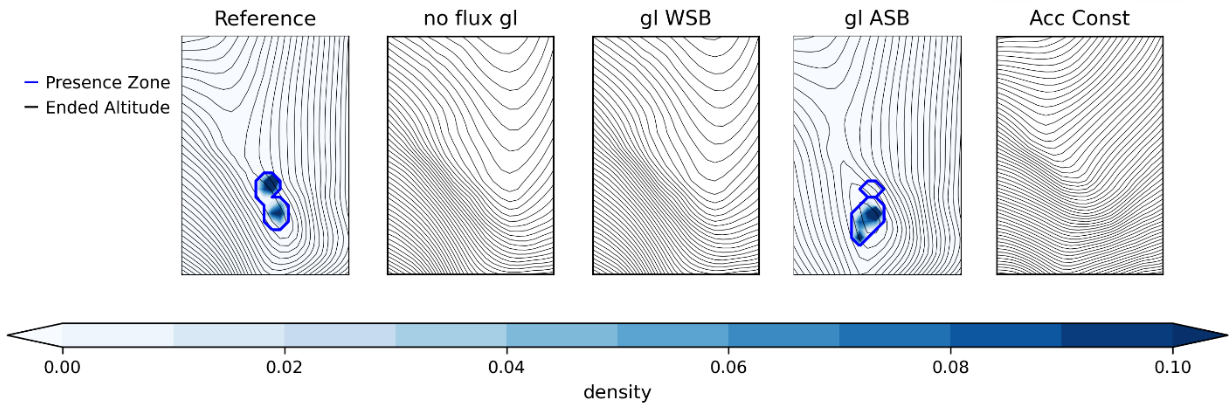

Figure 8: Density of presence over the 800,000 years is illustrated by the blue color bar for the reference simulation and for the three sensitivities tests. The blue contours represent the surface of presence during the simulation.

4 Discussions

Our study, simulating the evolution of the AIS over the past 800 kyr, demonstrates that the position of Dome C has not remained fixed over time, and that these displacements can introduce errors in the age–depth relationship of up to several hundred thousand years at the base of the ice core. This uncertainty is particularly critical in the context of the Beyond EPICA project, which aims to reconstruct a continuous climate record extending beyond one million years, as the base of the ice core represents precisely the most sensitive part of this record. Our sensitivity experiments further suggest that this displacement is primarily controlled by grounding-line dynamics in the Aurora Subglacial Basin, rather than by local changes in precipitation. This shows that better reconstructions of past grounding-line retreat and advance in this region, driven by ocean forcing, are needed. Coupled ice-sheet–ocean models could help reduce this source of chronological uncertainty. Future experiments using more realistic ocean forcing will be needed to better quantify the actual age error at the base of the ice core.

Moreover, to simulate ice sheet geometry changes over the last 800,000 years we had to make some simplifications of past climate change, which in turns could affect our results. First, we used an atmospheric index based on the EPICA Dome C ice core, and an oceanic index derived from a stack of sediment core (see section 2.2), to force GRISLI. In doing so, climate variations driven by these indices were applied uniformly across the entire model domain. According to several studies based on multiple Antarctic ice cores, temperature (Buizert et al., 2021; Bouchet et al., 2023) and precipitation (Parrenin et al., 2016) variations do not exhibit the same behavior across different locations. This spatial heterogeneity is also evident in marine sediment cores, where for example, Bates et al. (2014) highlighted significant differences in the timing and magnitude of warming depending on the coring site. It would therefore be valuable to repeat this study by applying region specific atmospheric and oceanic indices.

Uncertainties remain in reconstructing past climate, and these inevitably affect the dynamics of the grounding line and at the end the Dome C position. Here we only used two snapshots, PI and LGM, to produce the pattern of climate change from interglacial to glacial periods for the whole 800,000 years. This choice likely oversimplifies past climate change. Using multiple snapshots representative of different glacial and interglacial states could better capture the diversity of climate patterns through time, and thus produce more realistic spatial and temporal variations in the forcing. Incorporating additional constraints from field data on past grounding line positions into new experiments could help increase the accuracy of the simulations (e.g., Crotti et al., 2022).

Furthermore, we show that grounding line position has a non-negligible impact on Dome C location, and consequently on the uncertainty in the age-depth relationship. It therefore becomes important to reduce uncertainties related to the oceanic climate beneath ice shelves, as well as to the parameterisation of basal melting. Although Burgard et al. (2022) shows that a basal melt parameterisation with a quadratic dependence on ocean temperature provides a reasonable approximation, it would be valuable to repeat these experiments using more sophisticated parameterisations, such as PICO (Reese et al., 2018), which would allow for a better representation of refreezing processes and sub-shelf ocean circulation.

Finally, the use of the 1D ice flow model relies on an important assumption, namely that horizontal velocities are negligible compared to vertical velocities. Chung et al. (2025) demonstrated that 1D ice flow models cannot account for errors arising from horizontal velocities, unlike 2.5D flow-tube models, and showed that the basal ice of the Beyond EPICA Little Dome C

https://doi.org/10.5194/egusphere-2026-5288
Preprint. Discussion started: 24 September 2026

ice core likely originates from a region approximately 15 km upstream of the drill site, introducing an additional error in the age–depth relationship. This effect is not captured by the 1D model used here. However, we note that dome migration and horizontal advection are unlikely to act independently. As the dome shifts position through time, the upstream origin of basal ice itself changes accordingly, potentially compounding the two sources of error. The 1D age error presented here should therefore be regarded as a lower-bound, first-order estimate of the true age error arising from Dome C non-stationary position, rather than a full quantification of its combined effect with horizontal ice-flow advection.

5 Conclusions

This study aims to quantify the migration of Dome C over the past 800,000 years using the GRISLI ice sheet model. Our results show that Dome C undergoes substantial displacements through glacial and interglacial cycles. We show that these displacements have a non-negligible impact on the age-depth relationship, with basal melting playing a dominant role for old ice ages, and ice thickness variations contributing significantly throughout the entire ice core.

Moreover, a recurrent pattern emerges from our simulations in which Dome C systematically occupies preferential positions during glacial periods and shifts toward distinct preferential locations during interglacial periods.

Another key result of this work is the strong sensitivity of Dome C position to grounding line dynamics, particularly in the Aurora Subglacial Basin. Variations in grounding line extent appear to be the main driver of Dome C position, whereas changes in precipitation pattern play only a minor role.

These new results further support the use of ice sheet models that explicitly account for the displacement of Dome C when computing age-depth relationships for deep ice cores. A natural next step would be to integrate the dome migration from our simulations directly into age modelling frameworks, in order to quantify its net contribution to chronological uncertainties alongside other sources of error. Beyond the ice core community, the sensitivity of Dome C position to grounding line dynamics identified in this study also highlights the potential of using ice core records, or isochrone, as indirect constraints on past grounding line migrations, opening new perspectives for reconstructing the long-term evolution of the East Antarctic Ice Sheet.

Author contributions

"VvA, AQ and CD designed the experiments, and VvA carried them out. VvA and KJ developed the zoom model code and VvA performed the simulations. VvA prepared the manuscript with contributions from all co-authors."

https://doi.org/10.5194/egusphere-2026-5288
Preprint. Discussion started: 24 September 2026

Competing interests

The contact author has declared that none of the authors has any competing interests.

Disclaimer

Copernicus Publications remains neutral with regard to jurisdictional claims made in the text, published maps, institutional affiliations, or any other geographical representation in this paper. While Copernicus Publications makes every effort to include appropriate place names, the final responsibility lies with the authors. Views expressed in the text are those of the authors and do not necessarily reflect the views of the publisher.

Acknowledgements

We acknowledge the World Climate Research Programme's Working Group on Coupled Modelling, which is responsible for the Paleoclimate Modelling Intercomparison Project (PMIP) for producing and making available their model output. We would also like to thank Michiel Van den Broeke and, more broadly, the IMAU laboratory for providing us with the results of the RACMO2.4p1 model.

Financial support

This research is a part of the Beyond EPICA project funded by the Agence National de la Recherche (ANR-22-CE01-0024). Victor van Aalderen is funded by the French National Research Agency (Grant: ANR-22-CE01-0021). Also, this study has received funding from Agence Nationale de la Recherche - France 2030 as part of the PEPR TRACCS programme under grant number ANR-22-EXTR-0010

References

Abe-Ouchi, A., Saito, F., Kageyama, M., Braconnot, P., Harrison, S. P., Lambeck, K., Otto-Bliesner, B. L., Peltier, W. R., Tarasov, L., Peterschmitt, J.-Y., and Takahashi, K.: Ice-sheet configuration in the CMIP5/PMIP3 Last Glacial Maximum experiments, Geosci. Model Dev., 8, 3621–3637, https://doi.org/10.5194/gmd-8-3621-2015, 2015.

Adloff, M., Reick, C. H., and Claussen, M.: Earth system model simulations show different feedback strengths of the terrestrial carbon cycle under glacial and interglacial conditions, Earth Syst. Dynam., 9, 413–425, https://doi.org/10.5194/esd-9-413-2018, 2018.

Bates, S. L., Siddall, M., and Waelbroeck, C.: Hydrographic variations in deep ocean temperature over the mid-Pleistocene transition, Quaternary Science Reviews, 88, 147–158, https://doi.org/10.1016/j.quascirev.2014.01.020, 2014.

Bazin, L., Landais, A., Lemieux-Dudon, B., Toyé Mahamadou Kele, H., Veres, D., Parrenin, F., Martinerie, P., Ritz, C., Capron, E., Lipenkov, V., Loutre, M.-F., Raynaud, D., Vinther, B., Svensson, A., Rasmussen, S. O., Severi, M., Blunier, T., Leuenberger, M., Fischer, H., Masson-Delmotte, V., Chappellaz, J., and Wolff, E.: An optimized multi-proxy, multi-site Antarctic ice and gas orbital chronology (AICC2012): 120–800 ka, Clim. Past, 9, 1715–1731, https://doi.org/10.5194/cp-9-1715-2013, 2013.

Beckmann, A. and Goosse, H.: A parameterization of ice shelf–ocean interaction for climate models, Ocean Modelling, 5, 157–170, https://doi.org/10.1016/S1463-5003(02)00019-7, 2003.

Bentley, M. J., Ó Cofaigh, C., Anderson, J. B., Conway, H., Davies, B., Graham, A. G. C., Hillenbrand, C.-D., Hodgson, D. A., Jamieson, S. S. R., Larter, R. D., Mackintosh, A., Smith, J. A., Verleyen, E., Ackert, R. P., Bart, P. J., Berg, S., Brunstein, D., Canals, M., Colhoun, E. A., Crosta, X., Dickens, W. A., Domack, E., Dowdeswell, J. A., Dunbar, R., Ehrmann, W., Evans, J., Favier, V., Fink, D., Fogwill, C. J., Glasser, N. F., Gohl, K., Golledge, N. R., Goodwin, I., Gore, D. B., Greenwood, S. L., Hall, B. L., Hall, K., Hedding, D. W., Hein, A. S., Hocking, E. P., Jakobsson, M., Johnson, J. S., Jomelli, V., Jones, R. S., Klages, J. P., Kristoffersen, Y., Kuhn, G., Leventer, A., Licht, K., Lilly, K., Lindow, J., Livingstone, S. J., Massé, G., McGlone, M. S., McKay, R. M., Melles, M., Miura, H., Mulvaney, R., Nel, W., Nitsche, F. O., O'Brien, P. E., Post, A. L., Roberts, S. J., Saunders, K. M., Selkirk, P. M., Simms, A. R., Spiegel, C., Stolldorf, T. D., Sugden, D. E., Van Der Putten, N., Van Ommen, T., Verfaillie, D., Vyverman, W., Wagner, B., White, D. A., Witus, A. E., and Zwartz, D.: A community-based geological reconstruction of Antarctic Ice Sheet deglaciation since the Last Glacial Maximum, Quaternary Science Reviews, 100, 1–9, https://doi.org/10.1016/j.quascirev.2014.06.025, 2014.

Bouchet, M., Landais, A., Grisart, A., Parrenin, F., Prié, F., Jacob, R., Fourré, E., Capron, E., Raynaud, D., Lipenkov, V. Y., Loutre, M.-F., Extier, T., Svensson, A., Legrain, E., Martinerie, P., Leuenberger, M., Jiang, W., Ritterbusch, F., Lu, Z.-T., and Yang, G.-M.: The Antarctic Ice Core Chronology 2023 (AICC2023) chronological framework and associated timescale for the European Project for Ice Coring in Antarctica (EPICA) Dome C ice core, Clim. Past, 19, 2257–2286, https://doi.org/10.5194/cp-19-2257-2023, 2023.

Brondex, J., Gagliardini, O., Gillet-Chaulet, F., and Durand, G.: Sensitivity of grounding line dynamics to the choice of the friction law, J. Glaciol., 63, 854–866, https://doi.org/10.1017/jog.2017.51, 2017.

https://doi.org/10.5194/egusphere-2026-5288
Preprint. Discussion started: 24 September 2026

Buizert, C., Fudge, T. J., Roberts, W. H. G., Steig, E. J., Sherriff-Tadano, S., Ritz, C., Lefebvre, E., Edwards, J., Kawamura, K., Oyabu, I., Motoyama, H., Kahle, E. C., Jones, T. R., Abe-Ouchi, A., Obase, T., Martin, C., Corr, H., Severinghaus, J. P., Beaudette, R., Epifanio, J. A., Brook, E. J., Martin, K., Chappellaz, J., Aoki, S., Nakazawa, T., Sowers, T. A., Alley, R. B., Ahn, J., Sigl, M., Severi, M., Dunbar, N. W., Svensson, A., Fegyveresi, J. M., He, C., Liu, Z., Zhu, J., Otto-Bliesner, B. L., Lipenkov, V. Y., Kageyama, M., and Schwander, J.: Antarctic surface temperature and elevation during the Last Glacial Maximum, Science, 372, 1097–1101, https://doi.org/10.1126/science.abd2897, 2021.

Burgard, C., Jourdain, N. C., Reese, R., Jenkins, A., and Mathiot, P.: An assessment of basal melt parameterisations for Antarctic ice shelves, The Cryosphere, 16, 4931–4975, https://doi.org/10.5194/tc-16-4931-2022, 2022.

Chandler, D. M. and Langebroek, P. M.: Glacial–interglacial Circumpolar Deep Water temperatures during the last 800 000 years: estimates from a synthesis of bottom water temperature reconstructions, Clim. Past, 20, 2055–2080, https://doi.org/10.5194/cp-20-2055-2024, 2024.

Chung, A., Parrenin, F., Steinhage, D., Mulvaney, R., Martín, C., Cavitte, M. G. P., Lilien, D. A., Helm, V., Taylor, D., Gogineni, P., Ritz, C., Frezzotti, M., O’Neill, C., Miller, H., Dahl-Jensen, D., and Eisen, O.: Stagnant ice and age modelling in the Dome C region, Antarctica, The Cryosphere, 17, 3461–3483, https://doi.org/10.5194/tc-17-3461-2023, 2023.

Chung, A., Parrenin, F., Mulvaney, R., Vittuari, L., Frezzotti, M., Zanutta, A., Lilien, D. A., Cavitte, M. G. P., and Eisen, O.: Age, thinning and spatial origin of the Beyond EPICA ice from a 2.5D ice flow model, The Cryosphere, 19, 4125–4140, https://doi.org/10.5194/tc-19-4125-2025, 2025.

Crotti, I., Quiquet, A., Landais, A., Stenni, B., Wilson, D. J., Severi, M., Mulvaney, R., Wilhelms, F., Barbante, C., and Frezzotti, M.: Wilkes subglacial basin ice sheet response to Southern Ocean warming during late Pleistocene interglacials, Nat Commun, 13, 5328, https://doi.org/10.1038/s41467-022-32847-3, 2022.

Dufresne, J.-L., Foujols, M.-A., Denvil, S., Caubel, A., Marti, O., Aumont, O., Balkanski, Y., Bekki, S., Bellenger, H., Benshila, R., Bony, S., Bopp, L., Braconnot, P., Brockmann, P., Cadule, P., Cheruy, F., Codron, F., Cozic, A., Cugnet, D., de Noblet, N., Duvel, J.-P., Ethé, C., Fairhead, L., Fichefet, T., Flavoni, S., Friedlingstein, P., Grandpeix, J.-Y., Guez, L., Guilyardi, E., Hauglustaine, D., Hourdin, F., Idelkadi, A., Ghattas, J., Joussaume, S., Kageyama, M., Krinner, G., Labetoulle, S., Lahellec, A., Lefebvre, M.-P., Lefevre, F., Levy, C., Li, Z. X., Lloyd, J., Lott, F., Madec, G., Mancip, M., Marchand, M., Masson, S., Meurdesoif, Y., Mignot, J., Musat, I., Parouty, S., Polcher, J., Rio, C., Schulz, M., Swingedouw, D., Szopa, S.,

https://doi.org/10.5194/egusphere-2026-5288
Preprint. Discussion started: 24 September 2026

Talandier, C., Terray, P., Viovy, N., and Vuichard, N.: Climate change projections using the IPSL-CM5 Earth System Model: from CMIP3 to CMIP5, Clim Dyn, 40, 2123–2165, https://doi.org/10.1007/s00382-012-1636-1, 2013.

Goelzer, H., Nowicki, S., Payne, A., Larour, E., Seroussi, H., Lipscomb, W. H., Gregory, J., Abe-Ouchi, A., Shepherd, A., Simon, E., Agosta, C., Alexander, P., Aschwanden, A., Barthel, A., Calov, R., Chambers, C., Choi, Y., Cuzzone, J., Dumas, C., Edwards, T., Felikson, D., Fettweis, X., Golledge, N. R., Greve, R., Humbert, A., Huybrechts, P., Le clec'h, S., Lee, V., Leguy, G., Little, C., Lowry, D. P., Morlighem, M., Nias, I., Quiquet, A., Rückamp, M., Schlegel, N.-J., Slater, D. A., Smith, R. S., Straneo, F., Tarasov, L., van de Wal, R., and van den Broeke, M.: The future sea-level contribution of the Greenland ice sheet: a multi-model ensemble study of ISMIP6, The Cryosphere, 14, 3071–3096, https://doi.org/10.5194/tc-14-3071-2020, 2020.

Gulick, S. P. S., Shevenell, A. E., Montelli, A., Fernandez, R., Smith, C., Warny, S., Bohaty, S. M., Sjunneskog, C., Leventer, A., Frederick, B., and Blankenship, D. D.: Initiation and long-term instability of the East Antarctic Ice Sheet, Nature, 552, 225–229, https://doi.org/10.1038/nature25026, 2017.

Haeger, C., Petrunin, A. G., and Kaban, M. K.: Geothermal Heat Flow and Thermal Structure of the Antarctic Lithosphere, Geochem Geophys Geosyst, 23, e2022GC010501, https://doi.org/10.1029/2022GC010501, 2022.

Hajima, T., Watanabe, M., Yamamoto, A., Tatebe, H., Noguchi, M. A., Abe, M., Ohgaito, R., Ito, A., Yamazaki, D., Okajima, H., Ito, A., Takata, K., Ogochi, K., Watanabe, S., and Kawamiya, M.: Development of the MIROC-ES2L Earth system model and the evaluation of biogeochemical processes and feedbacks, Geosci. Model Dev., 13, 2197–2244, https://doi.org/10.5194/gmd-13-2197-2020, 2020.

Halberstadt, A. R. W. and Balco, G.: Antarctic ice sheet model comparison with uncurated geological constraints shows that higher spatial resolution improves deglacial reconstructions, The Cryosphere, 20, 931–961, https://doi.org/10.5194/tc-20-931-2026, 2026.

Hayden, A.-M., Pelle, T., and Dow, C. F.: The past, present, and future evolution of Aurora Subglacial Basin's subglacial drainage system, Nat Commun, 16, 2747, https://doi.org/10.1038/s41467-025-57700-1, 2025.

Jourdain, N. C., Asay-Davis, X., Hattermann, T., Straneo, F., Seroussi, H., Little, C. M., and Nowicki, S.: A protocol for calculating basal melt rates in the ISMIP6 Antarctic ice sheet projections, The Cryosphere, 14, 3111–3134, https://doi.org/10.5194/tc-14-3111-2020, 2020.

https://doi.org/10.5194/egusphere-2026-5288
Preprint. Discussion started: 24 September 2026

Jouzel, J., Masson-Delmotte, V., Cattani, O., Dreyfus, G., Falourd, S., Hoffmann, G., Minster, B., Nouet, J., Barnola, J. M., Chappellaz, J., Fischer, H., Gallet, J. C., Johnsen, S., Leuenberger, M., Loulergue, L., Luethi, D., Oerter, H., Parrenin, F., Raisbeck, G., Raynaud, D., Schilt, A., Schwander, J., Selmo, E., Souchez, R., Spahni, R., Stauffer, B., Steffensen, J. P., Stenni, B., Stocker, T. F., Tison, J. L., Werner, M., and Wolff, E. W.: Orbital and Millennial Antarctic Climate Variability over the Past 800,000 Years, Science, 317, 793–796, https://doi.org/10.1126/science.1141038, 2007.

Koutnik, M. R., Fudge, T. J., Conway, H., Waddington, E. D., Neumann, T. A., Cuffey, K. M., Buizert, C., and Taylor, K. C.: Holocene accumulation and ice flow near the West Antarctic Ice Sheet Divide ice core site, JGR Earth Surface, 121, 907–924, https://doi.org/10.1002/2015JF003668, 2016.

Lilien, D. A., Steinhage, D., Taylor, D., Parrenin, F., Ritz, C., Mulvaney, R., Martín, C., Yan, J.-B., O'Neill, C., Frezzotti, M., Miller, H., Gogineni, P., Dahl-Jensen, D., and Eisen, O.: Brief communication: New radar constraints support presence of ice older than 1.5 Myr at Little Dome C, The Cryosphere, 15, 1881–1888, https://doi.org/10.5194/tc-15-1881-2021, 2021.

Lliboutry, L.: A critical review of analytical approximate solutions for steady state velocities and temperatures in cold ice sheets, Z. Gletscherkd. Glazialgeol., 15(2), 135–148, 1979.

Ma, Y., Gagliardini, O., Ritz, C., Gillet-Chaulet, F., Durand, G., and Montagnat, M.: Enhancement factors for grounded ice and ice shelves inferred from an anisotropic ice-flow model, J. Glaciol., 56, 805–812, https://doi.org/10.3189/002214310794457209, 2010.

Marshall, S. J. and Cuffey, K. M.: Peregrinations of the Greenland Ice Sheet divide in the last glacial cycle: implications for central Greenland ice cores, Earth and Planetary Science Letters, 179, 73–90, https://doi.org/10.1016/S0012-821X(00)00108-4, 2000.

Mauritsen, T., Bader, J., Becker, T., Behrens, J., Bittner, M., Brokopf, R., Brovkin, V., Claussen, M., Crueger, T., Esch, M., Fast, I., Fiedler, S., Fläschner, D., Gayler, V., Giorgetta, M., Goll, D. S., Haak, H., Hagemann, S., Hedemann, C., Hohenegger, C., Ilyina, T., Jahns, T., Jimenéz-de-la-Cuesta, D., Jungclaus, J., Kleinen, T., Kloster, S., Kracher, D., Kinne, S., Kleberg, D., Lasslop, G., Kornblueh, L., Marotzke, J., Matei, D., Meraner, K., Mikolajewicz, U., Modali, K., Möbis, B., Müller, W. A., Nabel, J. E. M. S., Nam, C. C. W., Notz, D., Nyawira, S., Paulsen, H., Peters, K., Pincus, R., Pohlmann, H., Pongratz, J., Popp, M., Raddatz, T. J., Rast, S., Redler, R., Reick, C. H., Rohrschneider, T., Schemann, V., Schmidt, H., Schnur, R., Schulzweida, U., Six, K. D., Stein, L., Stemmler, I., Stevens, B., Storch, J., Tian, F., Voigt, A., Vrese, P., Wieners, K., Wilkenskjeld, S.,

https://doi.org/10.5194/egusphere-2026-5288
Preprint. Discussion started: 24 September 2026

Winkler, A., and Roeckner, E.: Developments in the MPI-M Earth System Model version 1.2 (MPI-ESM1.2) and Its Response to Increasing CO_2, J. Adv. Model. Earth Syst., 11, 998–1038, https://doi.org/10.1029/2018MS001400, 2019.

Morlighem, M.: MEaSUREs BedMachine Antarctica, Version 3, https://doi.org/10.5067/FPSU0V1MWUB6, 2022.

Mouginot, J., Rignot, E., Scheuchl, B., and Millan, R.: Comprehensive Annual Ice Sheet Velocity Mapping Using Landsat-8, Sentinel-1, and RADARSAT-2 Data, Remote Sensing, 9, 364, https://doi.org/10.3390/rs9040364, 2017.

Nereson, N. A., Raymond, C. F., Waddington, E. D., and Jacobel, R. W.: Migration of the Siple Dome ice divide, West Antarctica, J. Glaciol., 44, 643–652, https://doi.org/10.3189/S0022143000002148, 1998.

Paillard, D., Labeyrie, L., and Yiou, P.: Macintosh Program performs time-series analysis, EoS Transactions, 77, 379–379, https://doi.org/10.1029/96EO00259, 1996.

Parrenin, F., Rémy, F., Ritz, C., Siegert, M. J., and Jouzel, J.: New modeling of the Vostok ice flow line and implication for the glaciological chronology of the Vostok ice core, J. Geophys. Res., 109, 2004JD004561, https://doi.org/10.1029/2004JD004561, 2004.

Parrenin, F., Dreyfus, G., Durand, G., Fujita, S., Gagliardini, O., Gillet, F., Jouzel, J., Kawamura, K., Lhomme, N., Masson-Delmotte, V., Ritz, C., Schwander, J., Shoji, H., Uemura, R., Watanabe, O., and Yoshida, N.: 1-D-ice flow modelling at EPICA Dome C and Dome Fuji, East Antarctica, Clim. Past, 3, 243–259, https://doi.org/10.5194/cp-3-243-2007, 2007.

Parrenin, F., Fujita, S., Abe-Ouchi, A., Kawamura, K., Masson-Delmotte, V., Motoyama, H., Saito, F., Severi, M., Stenni, B., Uemura, R., and Wolff, E. W.: Climate dependent contrast in surface mass balance in East Antarctica over the past 216 ka, J. Glaciol., 62, 1037–1048, https://doi.org/10.1017/jog.2016.85, 2016.

Parrenin, F., Cavitte, M. G. P., Blankenship, D. D., Chappellaz, J., Fischer, H., Gagliardini, O., Masson-Delmotte, V., Passalacqua, O., Ritz, C., Roberts, J., Siegert, M. J., and Young, D. A.: Is there 1.5-million-year-old ice near Dome C, Antarctica?, The Cryosphere, 11, 2427–2437, https://doi.org/10.5194/tc-11-2427-2017, 2017.

Pollard, D. and DeConto, R. M.: Description of a hybrid ice sheet-shelf model, and application to Antarctica, Geosci. Model Dev., 5, 1273–1295, https://doi.org/10.5194/gmd-5-1273-2012, 2012.

https://doi.org/10.5194/egusphere-2026-5288
Preprint. Discussion started: 24 September 2026

Quiquet, A., Dumas, C., Ritz, C., Peyaud, V., and Roche, D. M.: The GRISLI ice sheet model (version 2.0): calibration and validation for multi-millennial changes of the Antarctic ice sheet, Geosci. Model Dev., 11, 5003–5025, https://doi.org/10.5194/gmd-11-5003-2018, 2018.

Quiquet, A., Roche, D. M., Dumas, C., Bouttes, N., and Lhardy, F.: Climate and ice sheet evolutions from the last glacial maximum to the pre-industrial period with an ice-sheet–climate coupled model, Clim. Past, 17, 2179–2199, https://doi.org/10.5194/cp-17-2179-2021, 2021.

Reese, R., Albrecht, T., Mengel, M., Asay-Davis, X., and Winkelmann, R.: Antarctic sub-shelf melt rates via PICO, The Cryosphere, 12, 1969–1985, https://doi.org/10.5194/tc-12-1969-2018, 2018.

Schoof, C.: Ice sheet grounding line dynamics: Steady states, stability, and hysteresis, J. Geophys. Res., 112, F03S28, https://doi.org/10.1029/2006JF000664, 2007.

Sepulchre, P., Caubel, A., Ladant, J.-B., Bopp, L., Boucher, O., Braconnot, P., Brockmann, P., Cozic, A., Donnadieu, Y., Dufresne, J.-L., Estella-Perez, V., Ethé, C., Fluteau, F., Foujols, M.-A., Gastineau, G., Ghattas, J., Hauglustaine, D., Hourdin, F., Kageyama, M., Khodri, M., Marti, O., Meurdesoif, Y., Mignot, J., Sarr, A.-C., Servonnat, J., Swingedouw, D., Szopa, S., and Tardif, D.: IPSL-CM5A2 – an Earth system model designed for multi-millennial climate simulations, Geosci. Model Dev., 13, 3011–3053, https://doi.org/10.5194/gmd-13-3011-2020, 2020.

Seroussi, H., Nowicki, S., Payne, A. J., Goelzer, H., Lipscomb, W. H., Abe-Ouchi, A., Agosta, C., Albrecht, T., Asay-Davis, X., Barthel, A., Calov, R., Cullather, R., Dumas, C., Galton-Fenzi, B. K., Gladstone, R., Golledge, N. R., Gregory, J. M., Greve, R., Hattermann, T., Hoffman, M. J., Humbert, A., Huybrechts, P., Jourdain, N. C., Kleiner, T., Larour, E., Leguy, G. R., Lowry, D. P., Little, C. M., Morlighem, M., Pattyn, F., Pelle, T., Price, S. F., Quiquet, A., Reese, R., Schlegel, N.-J., Shepherd, A., Simon, E., Smith, R. S., Straneo, F., Sun, S., Trusel, L. D., Van Breedam, J., van de Wal, R. S. W., Winkelmann, R., Zhao, C., Zhang, T., and Zwinger, T.: ISMIP6 Antarctica: a multi-model ensemble of the Antarctic ice sheet evolution over the 21st century, The Cryosphere, 14, 3033–3070, https://doi.org/10.5194/tc-14-3033-2020, 2020.

Stefanini, C., Stenni, B., Masiol, M., Dreossi, G., Favier, V., Becherini, F., Scarchilli, C., Ciardini, V., Carugati, G., and Frezzotti, M.: Challenges in surface mass balance estimation at Dome C: stake farm comparisons, measurement uncertainties, and station-induced biases, The Cryosphere, 19, 5781–5799, https://doi.org/10.5194/tc-19-5781-2025, 2025.

Sueyoshi, T., Ohgaito, R., Yamamoto, A., Chikamoto, M. O., Hajima, T., Okajima, H., Yoshimori, M., Abe, M., O'ishi, R., Saito, F., Watanabe, S., Kawamiya, M., and Abe-Ouchi, A.: Set-up of the PMIP3 paleoclimate experiments conducted using an Earth system model, MIROC-ESM, Geosci. Model Dev., 6, 819–836, https://doi.org/10.5194/gmd-6-819-2013, 2013.

Sutter, J., Fischer, H., Grosfeld, K., Karlsson, N. B., Kleiner, T., Van Liefferinge, B., and Eisen, O.: Modelling the Antarctic Ice Sheet across the mid-Pleistocene transition – implications for Oldest Ice, The Cryosphere, 13, 2023–2041, https://doi.org/10.5194/tc-13-2023-2019, 2019.

Tarasov, L. and Richard Peltier, W.: Greenland glacial history and local geodynamic consequences, Geophysical Journal International, 150, 198–229, https://doi.org/10.1046/j.1365-246X.2002.01702.x, 2002.

Tarasov, L., Dyke, A. S., Neal, R. M., and Peltier, W. R.: A data-calibrated distribution of deglacial chronologies for the North American ice complex from glaciological modeling, Earth and Planetary Science Letters, 315–316, 30–40, https://doi.org/10.1016/j.epsl.2011.09.010, 2012.

Ullman, D. J., LeGrande, A. N., Carlson, A. E., Anslow, F. S., and Licciardi, J. M.: Assessing the impact of Laurentide Ice Sheet topography on glacial climate, Clim. Past, 10, 487–507, https://doi.org/10.5194/cp-10-487-2014, 2014.

Urbini, S., Frezzotti, M., Gandolfi, S., Vincent, C., Scarchilli, C., Vittuari, L., and Fily, M.: Historical behaviour of Dome C and Talos Dome (East Antarctica) as investigated by snow accumulation and ice velocity measurements, Global and Planetary Change, 60, 576–588, https://doi.org/10.1016/j.gloplacha.2007.08.002, 2008.

Van Aalderen, V., Charbit, S., Dumas, C., and Quiquet, A.: Relative importance of the mechanisms triggering the Eurasian ice sheet deglaciation in the GRISLI2.0 ice sheet model, Clim. Past, 20, 187–209, https://doi.org/10.5194/cp-20-187-2024, 2024.

Van Dalum, C. T., Van De Berg, W. J., Van Den Broeke, M. R., and Van Tiggelen, M.: The surface mass balance and near-surface climate of the Antarctic ice sheet in RACMO2.4p1, The Cryosphere, 19, 4061–4090, https://doi.org/10.5194/tc-19-4061-2025, 2025.

Vittuari, L., Zanutta, A., Gandolfi, S., Martelli, L., Ritz, C., Urbini, S., and Frezzotti, M.: Decadal migration of Dome C inferred by global navigation satellite system measurements, J. Glaciol., 71, e117, https://doi.org/10.1017/jog.2025.28, 2025.

Voldoire, A., Sanchez-Gomez, E., Salas y Mélia, D., Decharme, B., Cassou, C., Sénési, S., Valcke, S., Beau, I., Alias, A., Chevallier, M., Déqué, M., Deshayes, J., Douville, H., Fernandez, E., Madec, G., Maisonnave, E., Moine, M.-P., Planton, S., Saint-Martin, D., Szopa, S., Tyteca, S., Alkama, R., Belamari, S., Braun, A., Coquart, L., and Chauvin, F.: The CNRM-CM5.1 global climate model: description and basic evaluation, Clim Dyn, 40, 2091–2121, https://doi.org/10.1007/s00382-011-1259-y, 2013.

Yukimoto, S., Adachi, Y., Hosaka, M., Sakami, T., Yoshimura, H., Hirabara, M., Tanaka, T. Y., Shindo, E., Tsujino, H., Deushi, M., Mizuta, R., Yabu, S., Obata, A., Nakano, H., Koshiro, T., Ose, T., and Kitoh, A.: A New Global Climate Model of the Meteorological Research Institute: MRI-CGCM3 —Model Description and Basic Performance—, Journal of the Meteorological Society of Japan, 90A, 23–64, https://doi.org/10.2151/jmsj.2012-A02, 2012.

Zheng, W. and Yu, Y.: Paleoclimate simulations of the mid-Holocene and last glacial maximum by FGOALS, Adv. Atmos. Sci., 30, 684–698, https://doi.org/10.1007/s00376-012-2177-6, 2013.